Measurements and Interpretation of Near-IR Spectra of Satellites

Eric C. Pearce, Harrison Krantz, Adam Block, and Mitchell Kirshner
University of Arizona

Liam O. Gunter
United States Naval Observatory

Brad Sease
Computational Physic Inc.

ABSTRACT

The characterization of deep space debris poses a significant challenge in Space Domain Awareness (SDA). Multi-color photometry and the resultant color indices offer the potential to rapidly discriminate between debris and intact space objects such as rocket bodies and satellites. These multi-color techniques can also identify anomalous members of object groups and cue higher fidelity data collections and studies. However, multi-color photometry can be difficult to interpret, as the effects of phase and rotation become conflated with the more fundamental material properties of the satellite, and the broad astronomical photometric bands may not identify key spectral features that can be diagnostic for SDA application.

In our previous measurements with the United Kingdom Infrared Telescope (UKIRT) Wide Field Camera (WFCAM), we characterized a wide range of space objects with the goal of developing techniques to rapidly discriminate between different classes of objects and to identify anomalous members of these groups. To date, our survey with WFCAM has produced a comprehensive database of 5-color photometry in the Z, Y, J, H, and K bands, analogous to the bands that are anticipated to be exploited by future U.S. ground-based SDA systems. Our current data set includes:

(a) Centaur rocket bodies (RBs)
(b) Molniya communication satellites including the -1K, 1T, -2, and -3 variants
(c) Russian FREGAT and SL-6 upper stage RBs in Molniya orbits
(d) Russian Breeze-M RB disposed in GEO-crossing graveyard like orbits, and the Angara-5/Breeze-M mass simulator, also disposed in a near-GEO orbit
(e) Intact payloads selected from satellites using the Boeing HS-376 busses—including four different generations of solar panel technology
(f) Special interest objects, including the JWST and the Chang-e 5 orbiter

During the spring of 2022, we made additional spectral measurements of many of these objects with the UKIRT 1-5 μm Imager-Spectrometer (UIST), providing high fidelity reflectance spectra to better inform our interpretation and analysis of the 5-color photometric measurements. These measurements constitute the most comprehensive collection of near-IR spectra of space objects that have been published. Our targets for UIST observation were carefully selected to include a mix of each of our ensemble groups. The fusion of this data with the previous 5-color photometry in the same bands is a unique opportunity to interpret the 5-color photometry in the context of the higher resolution spectra. Our measurements of the recently launched James Webb Space Telescope (JWST) with both WFCAM and with UIST establishes a baseline spectrum of the JWST sunshade and we anticipate monitoring this object carefully in coming campaigns to study the evolution of its reflectance spectra with time.

1. INTRODUCTION

Since the launch of Sputnik in 1957, space surveillance has tracked and studied satellites and space debris with optical telescopes. The first attempts to use optical photometry to characterize satellites were published by the U.S and Russians in the late 1950s [1, 2]. The excellent historical review papers by Lambert [3] and Sukhov [4] summarize much of the history of photometric technique development in the US and Russia respectively. Multi-color photometric measurements offer the opportunity to quickly measure the bulk spectral characteristics of a space object. The concept of exploiting the color indices in the visible bands has been previously explored in SSA. For

example, Lederer et al. used BVRI photometry from the Cerro Tololo Inter-American Observatory (CTIO) 0.9 m telescope to compare measured color indices of 18 IDCSP (Initial Defense Communications Satellite Program) satellites with the predictions from laboratory measurements of solar cells [5]. Frith et al. previously measured a selection of objects with UKIRT WFCAM and documented phase angle variation on the J-K and H-K color indices. Phase angle variations in J-K and H-K scaled order of 0.2 to 0.3 magnitudes, and although the satellites shared some common trends, each displayed its own unique characteristic [6].

During late 2020 and early 2021, our team using the United Kingdom Infrared Telescope (UKIRT) expanded upon our previous 2016–2017 characterization survey [7]. These measurements used the unique Wide Field CAMera (WFCAM) that operates at the prime focus [8]. More recently, our measurements utilized the recently recommissioned Cassegrain spectrometers, the UKIRT 1-5 μm Imager-Spectrometer (UIST) and the Michelle mid-infrared imaging spectrometer which operates from 8-25 μm [9, 10]. The UIST spectrometer covers the 1-5 μm near-infrared and overlaps the spectral coverage available with the WFCAM. UIST supports both an imaging mode with a maximum field of view (FOV) of approximately 2 arcminutes, and a 9-slot grism wheel allowing the observer to select the bandwidth and spectral resolution desired. For our measurements, we used the IJ (0.862-1.418 μm) and the HK (1.395-2.506 μm) to provide maximal overlap with our supporting five-color photometric measurements with WFCAM in the Z, Y , J, H, and K bands. During the summer 2022 campaign we also attempted measurements with the Michelle mid-infrared spectrometer. However, throughput issues with the Michelle window limited possible observations to only broadband photometric measurements in imaging mode. We will report these measurements will in a separate publication.

Compared to multi-color photometric measurements, there are relatively few spectral measurements in either the visible or infrared of satellites published in the open literature. This is largely driven by the relatively difficult measurement techniques and instrumentation required to make such measurements. Due to the higher spectral resolution, larger telescopes are required. Moreover, calibration and data reduction are significantly more difficult. Nonetheless, spectral measurements can be used to identify specific spacecraft materials by directly observing absorption features of those materials. In particular, the mid-IR absorption features of solar panels near 2.3 and 2.37 μm are especially prominent in both our data and previous studies [11, 12]. Other researchers have published visible spectra of satellites using the 6.5 m Walter Baade Magellan telescope [13], the 3.67 m AMOS telescope [14], the 1 m ESA Space Debris Telescope [15], and the 6.5 m MMT telescope [16]. Nonetheless, the collection of complete, well-calibrated satellite spectra is very limited. In previous unpublished research, the Justice Bruursema measured a collection of Titan 3C and Breeze-M rocket bodies and other objects with UIST and the methods documented were a valuable resource in our data reduction.

In this paper we focus on our recent results with the HS-376 busses, highlighting the ability of near-IR photometry to distinguish between the subtle differences in solar panel material between different models. These initial results also highlight some of the challenges of applying UKIRT and near-IR photometry for SSA characterization, including deconvolving the various factors such as phase angle, rotation, and pose that all effect both color and brightness during the collection.

2. STUDY TARGET ENSEMBLES

This paper focuses on the recent measurements of satellites based on the HS-376 bus. The HS-376 satellite bus was a common communications satellite bus introduced in 1978. A total of 58 HS-376 based satellites were launched from 1978 to 2003. The satellite bus features a cylindrical body with two sections one of which nests inside the other and extends out when in orbit (see Figure 1). The cylindrical body is 2.2 m in diameter and when extended between 6.5 m and 7 m long. The exterior surface is almost completely covered in solar cells and is otherwise largely featureless. The main body of the spacecraft is spin-stabilized at 50 rpm and the payload shelf despun to provide radio antenna pointing. At end-of-life the spin-rate is no longer maintained and the despun section becomes coupled with the rest of the satellite. The transfer of inertia from the body to the previously despun mass results in a reduction of the overall spin rate compared to the operational spin rate.

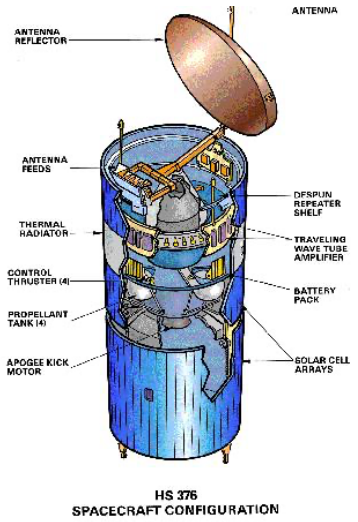

Figure 1. Drawing of the HS-376 satellite bus.

There are four major variations to the design of the HS-376: the standard HS-376, the long-life HS-376L, the higher-powered HS-376HP, and the larger HS-376W. Only the HS-376W featured a notably different bus with a larger diameter cylindrical body. Only four of the HS-376W were launched. During the twenty-year evolution of the HS-376, the solar cell technology was incrementally upgraded for new satellites. The majority of HS-376 satellites utilized silicon-based solar cells including K4 ¾ and K7 varieties. The most modern HS-376 satellites utilized GaAs-based solar cells.

3. CURRENT MEASURMENTS

For this observing campaign with UIST we followed the established procedures utilized for astronomical targets. This relatively time-consuming procedure involves for each target: slewing to the target position, recording calibration flat and arc images, searching for and slewing to a nearby standard star, centering the standard star on the science detector, recording spectra of the standard star, slewing back to the target, centering the target on the science detector, and finally recording spectra of the science target. We experienced additional difficulty because our targets are satellites and the current systems do not easily accommodate non-sideral targets. Due to unpredictable scheduling of satellite observations we did not pre-select standard stars and instead searched for suitable nearby standard stars at the time of observation. When searching for an appropriate standard star we looked for solar analog (G type) of 9-11th visual magnitude. These calibration stars were bright enough to yield a high SNR but not too bright to saturate the detector during acquisition.

The most time-consuming step in the procedure was finding the target satellite and centering it on the science detector. UIST has a small 2 arcmin FOV and the target satellite rarely appeared in the FOV without a tedious grid search. Additionally due to tracking difficulties the target satellite often drifted off the slit requiring us to stop science exposures and reacquire the target before resuming recording spectra.

For each individual target we recorded spectra with both the IJ and HK grisms which cover the 0.862 – 1.418 μm and 1.395 – 2.506 μm wavelengths respectively. For all observations we utilized the 4-pixel wide (0.48 arcsec) slit which yields spectral resolution of R=320 with the IJ grism and R=500 with the HK grism. We recorded multiple consecutive 60 seconds or longer exposures for each target following an ABBA nodding pattern for sky subtraction. Multiple recorded spectra are summed together to increase the overall SNR.

We processed the data following the established procedures for UIST data. This utilizes the Starlink software and ORAC-DR reduction pipeline [20, 21]. In principle, the reduction pipeline produces calibrated spectra with real flux units of $W/m^2/\mu m$ determined from the observed standard star and cataloged magnitude. However, during our observations, difficulties in tracking and auto-guiding caused the target satellite to often drift off the slit. This means we cannot know for how long the satellite was observed through the slit during a given exposure time and cannot rely on the calibrated measurements to be a true measure of brightness. This phenomenon is most readily seen as a variation in mean measured flux from one spectrum to the next, and different measured flux for the two IJ and HK bands.

To normalize and match the IJ and HK spectra together we calculated the mean flux value over the wavelength range where the two bands overlap, 1.395 – 1.420 μm, and then scale the two spectra to match. This is a very

small wavelength range to match with and is within the atmospheric water vapor absorption region. Although telluric correction with a standard star restores this part of the spectrum, low SNR after correction makes this a nonideal wavelength for matching. Nonetheless this simple scaling and matching method works in most cases.

Table 1 lists six different HS-376 satellites which we observed with UIST during our campaign. These include both satellites with silicon-based solar cells and GaAs-based solar cells. We additionally determined the rotational period for each satellite from accompanying observations with the Chimera high-speed photometer which we operate on the Kuiper 61 inch telescope near Tucson, AZ [22, 23]. Figure 2 shows the light curve of Galaxy 3, one of the HS-376 satellites we observed. The HS-376 satellites all have rotational periods of a few seconds thus our 60 second exposures with UIST are effectively averaged over many rotations. During the 1-2 hrs required to observe in both the IJ and HK grisms the target satellite phase angle changes. The average observed phase angle for each target is listed.

Table 1. *The details of the observed HS-376 bus satellites. The rotational period is measured from light curves created with the Chimera high-speed photometer. The phase angle is the average during the 1-2 hrs required for observing with both the IJ and HK grisms*

SATCAT ID	NAME	LAUNCH YEAR	SOLAR ARRAY TYPE	ROTATIONAL PERIOD	AVG. OBSERVED PHASE ANGLE
15308	Galaxy 3	1984	Silicon K7 & K4 3/4	1.8 s	36.7 deg for IJ 103.5 deg for HK
21906	Galaxy 5	1992	Silicon K7	2.7 s	17.2 deg
22931	Thaicom 1A	1993	Silicon	2.7 s	38.5 deg
23943	Apstar 1A	1996	Silicon K4 3/4	3.0 s	14.2 deg
25358	Thor 3	1998	GaAs	3.2 s	30.8 deg
25546	Bonum 1	1998	GaAs	3.1 s	42.5 deg

Figure 3 shows the calibrated and scaled spectra for the six different HS-376 satellites. All the satellites exhibit a generally downward sloping spectrum following that of a solar spectrum as is expected since this is reflected sunlight. The two prominent atmospheric water vapor regions (1.35 – 1.5 μm & 1.8 – 2.0 μm) are shaded in gray and any apparent features in these regions should be ignored or interpreted carefully. All four HS-376 satellites with silicon-based solar cells exhibit similar spectra with a characteristic peak near 1.1 μm. This is notably different from the two satellites with GaAs-based solar cells which peak near 1.0 μm and exhibit a broader hump from 0.9 μm to 1.3 μm.

Figure 4 shows the reflected spectra for the same six HS-376 satellites. The reflected spectra is the scaled spectra divided by a reference solar spectrum. In principle an ideal colorless gray satellite would exhibit a flat reflected spectrum. Any deviations from a flat spectrum are thus indicative of the color and materials of the observed satellite. Most importantly, we can directly compare the reflected spectra to lab measurements of specific materials. In particular, we compare the observed spectra to the lab measurements of the same silicon solar cells and GaAs solar cells made by Reyes [24]. Our observed spectra of HS-376 satellites with silicon-based solar cells closely match the lab measurements of the same silicon solar cells. Both exhibit a rise in reflectance from 1.0 μm to 1.1 μm, and a generally flat spectrum up to 2.5 μm. The lab measurements show clear absorption features at approximately 1.7, 1.75, 2.3, and 2.37 μm. The cleaner, higher-SNR spectra, particularly the spectrum of Apstar 1A, exhibit the same absorption features.

Curiously our two observed spectra of HS-376 satellites with GaAs-based solar cells differ greatly from the lab measurements of the same GaAs solar cells. The lab measurements show low reflectance below 1.5 μm and a gradual rise in reflectance from 1.5 to 2.1 μm. Our observed spectra show significant reflectance between 0.9 μm and 1.3 μm where we'd expect very little based on the lab measurements. The observed spectrum of Thor 3 does show a gradual rise from 1.5 to 2.1 μm which matches the lab measurements. The observed spectrum of Bonum 1 shows a similar but more subtle rise from 1.5 to 2.1 μm and with an intermediate dip around 1.65 μm. The lab measurements of GaAs solar cells show the same 2.3 and 2.37 μm absorption features as the silicon solar cells. The spectrum of Bonum 1 also exhibits these absorption features. The spectrum of Thor 3 may include these as well but not as clearly.

To explain the 0.9 – 1.3 μm hump we see in the spectra of the two HS-376 satellites with GaAs-based solar cells we must understand that we are not only observing the solar array but a combination of reflected light from all parts of the satellite. The exterior of the HS-376 satellite bus is almost completely covered in solar cells which is one reason why we chose them for study. However, the high-resolution light curves, an example shown in Figure 2, produced from our accompanying high-speed photometric observations reveal that the overall averaged brightness is dominated by bright periodic specular reflections. The specular reflections are not from the solar cells which are uniformly wrapped around the spinning cylindrical body as this would not produce periodic reflections. Our interpretation of the light curve is the specular reflections are from the face, back, and sides of the flat antenna reflector. If the specular reflections from of the antenna reflector are dominating the overall brightness, then our rotationally averaged spectra are really spectra of the antenna reflector with the solar array in the background. We do not have concrete information regarding the materials of the antenna reflector. However historical photos of one HS-376 satellite bus show the antenna reflector is wrapped in some type of metalized film and the face is a mirror-like, tensioned film.

If the 0.9 – 1.3 μm hump is from the antenna reflector then we would expect to see this same hump in all observed HS-376 satellites. However, none of the observed HS-376 satellites with silicon-based solar cells exhibit the hump. There are multiple possible explanations for this discrepancy. Firstly, the reflections from the antenna reflector are specular and their visibility dependent on the observation geometry and pose of the satellite. Thus not every satellite in every geometry is going to appear the same. Secondly, the GaAs-based solar cells are overall less reflective than the silicon-based solar cells. Thus, the reflections from the antenna reflector will be relatively brighter than the GaAs-based solar cells and more apparent than the silicon-based solar cells. Lastly, since we do not have concrete information about the materials of the antenna reflector, we also do not know if the construction is consistent over the many models of the HS-376. Based on some of the artistic imagery we have reason to think it changed from satellite to satellite. We also must consider aging and the resultant change in materials in the harsh space environment. The large number of HS-376 satellites and range in launch dates create an ideal ensemble for investigating aging which we intend to continue considering in our study of satellite spectra.

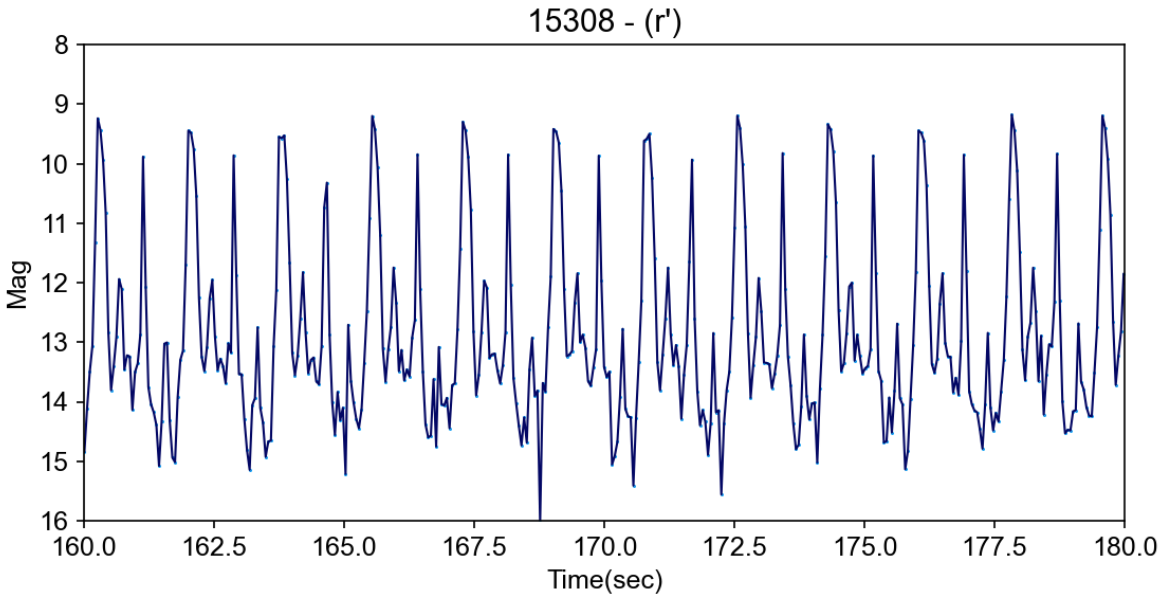

Figure 2. The light curve of Galaxy 3 (15308) shows a four-peaked period typical to all HS-376 satellites. We think the bright specular reflections are from the face, back, and sides of the antenna reflector. These bright reflections dominate the overall brightness of the satellite. This light curve is created with high-speed photometry recorded with Chimera on the Kuiper 61 inch telescope.

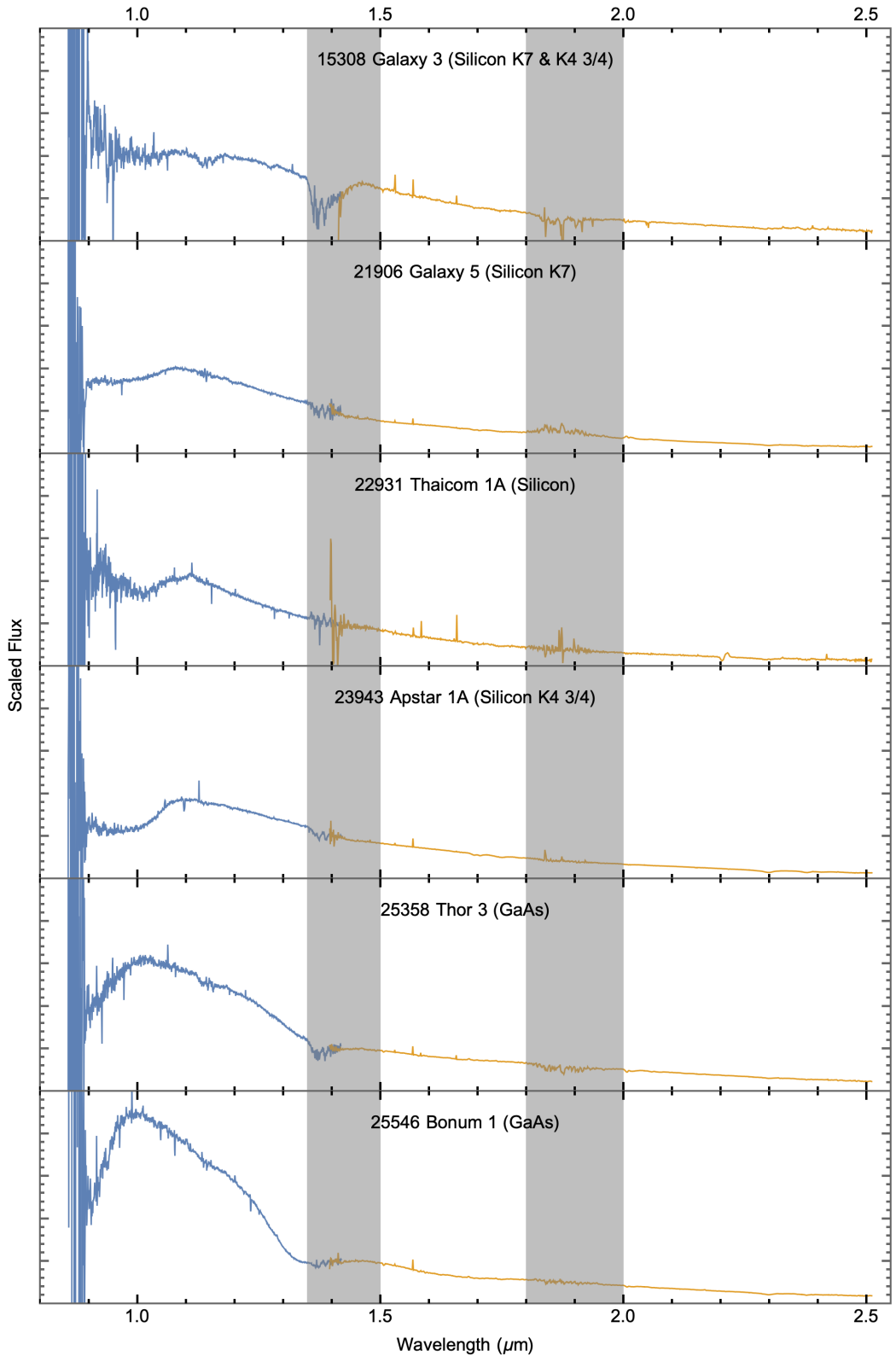

Figure 3. The calibrated from 0.9 - 2.5 μm spectra for several HS-376 satellites. For each target the separate IJ and HK spectra are scaled such that the mean flux is the same for 1.395 – 1.42 μm where the two bands overlap. The prominent water vapor absorption regions are shaded in gray.

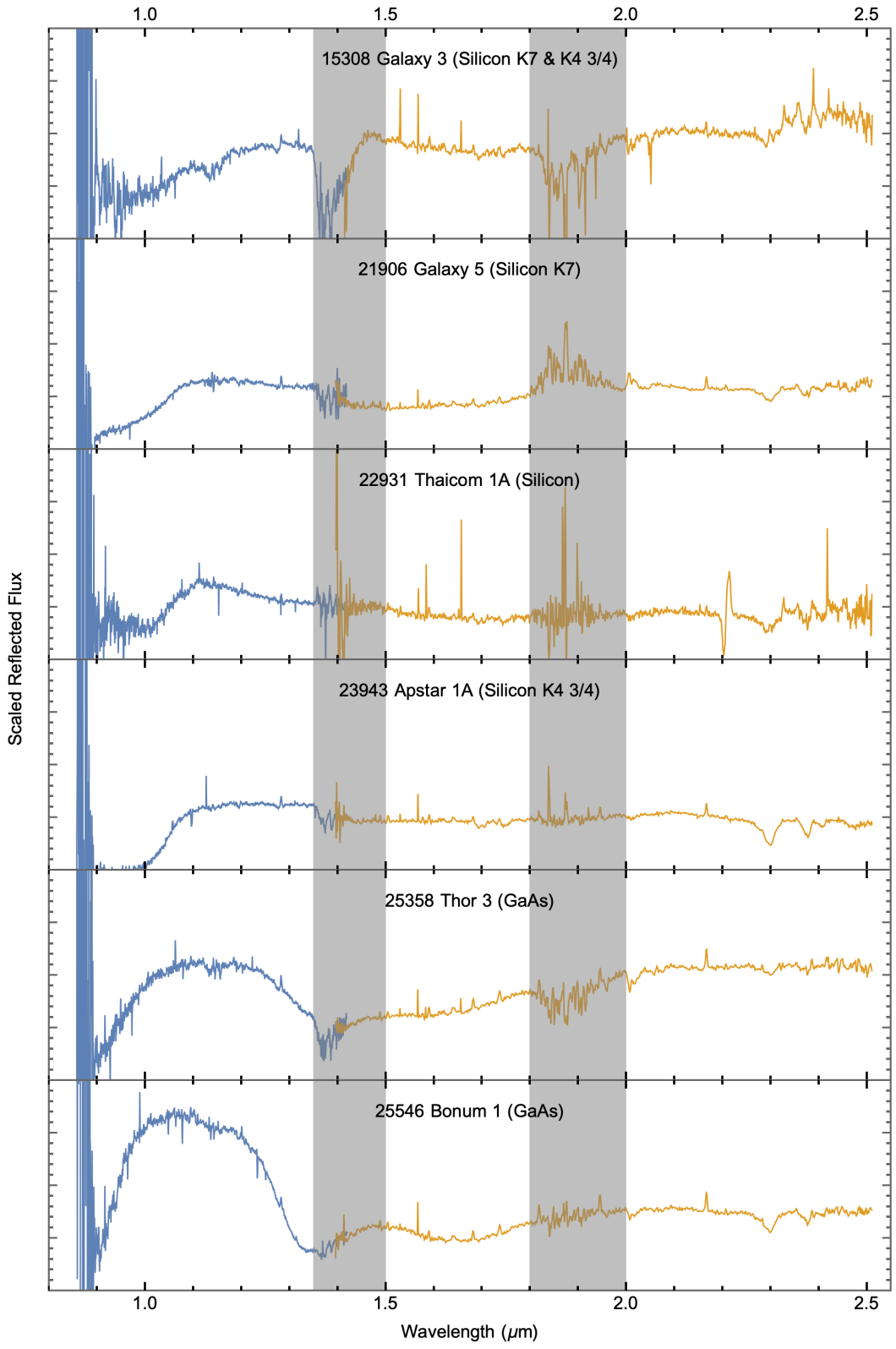

Figure 4. The reflected from 0.9 - 2.5 μm spectra for several HS-376 satellites. The reflected spectra is created by dividing the calibrated spectra by a reference solar spectrum. The prominent water vapor absorption regions are shaded in gray.

4. SUMMARY AND FUTURE OBSERVATIONS

In the spring of 2022 we observed a number of satellites with UIST to create near-IR spectra. In particular we observed several different HS-376 satellites including models with silicon-based solar cells and others with GaAs-based solar cells. The HS-376 satellites with silicon-based solar cells exhibited relatively flat reflectance spectra with absorption features that closely match the lab measurements of the same solar cells. The HS-376 satellites with GaAs-based solar cells match the lab measurements above 1.5 μm including absorption features, but also show a significant increase in reflectance from 0.9 – 1.3 μm which is not seen in the lab measurements. We explain this discrepancy as a result of spectral mixing with bright specular reflections from the antenna reflector. Our accompanying high-resolution light curves show that for HS-376 satellites the overall averaged brightness is dominated by specular reflections.

During our first observing campaign using UIST we experienced many challenges and difficulties. The existing systems and procedures are intended for astronomical studies and not well tailored for measurements of non-sidereal satellites. The already time-consuming series of steps required to create high-quality spectra are further slowed by the challenges of non-sidereal observing, especially the challenge of accurate tracking to keep the target satellite on the slit. Compared to photometry, spectroscopy requires more complicated instrumentation and operations. Additionally, spectroscopy is infamously inefficient with low throughput requiring large telescopes and multiple long exposures. During our observing with UIST each target required minimum 1-2 hrs to acquire and record spectra. Nonetheless, the higher resolution spectra offers greater insights into specific material composition of the reflecting surfaces that multi-color photometry cannot provide.

5. ACKNOWLEDGEMENTS

This work was funded by the United States Naval Observatory in support of ongoing research and development in the area of orbital debris detection and tracking, and by the University of Arizona Office of Research, Discovery and Innovation.

Supporting observations reported here were obtained with the Kuiper 61” Telescope operated by the University of Arizona Steward Observatory. The Chimera Photometer was developed with funding the University of Arizona Office of Research, Discovery, and Innovation. Dr. Pearce has a financial conflict of interest that is being managed by the University of Arizona in accordance with its policies.

6. REFERENCES

1. J. G. Moore (1959), "Photometric Observations of the Second Soviet Satellite (1957 β1)," *Publications of the Astronomical Society of the Pacific*, vol. 71, (419), pp. 163–165.
2. V. M. Grigorevskij (1959), “About Methods of Photometry of Artificial Earth’s Satellites,” Byulleten' Stantsii Nablyudenia ISZ, No. 7, p. 14.
3. J. V. Lambert and K.E. Kissell (2006), “The Early Development of Satellite Characterization Capabilities at the Air Force Laboratories,” in Proceedings AMOS Conference, Wailea, Maui, Hawaii.
4. P. P. Sukhov and K. P. Sukhov (2015), "On some problems of photometric identification of geostationary satellites," Kinematics and Physics of Celestial Bodies, vol. 31, (6), pp. 314–318.
5. S.M. Lederer et al (2012), “Preliminary Characterization of IDCSP Spacecrafts through a Multi-Analytical Approach,” in Proceedings AMOS Conference, Wailea, Maui, Hawaii.
6. J. Frith, P. Anz-Meador, S. Lederer, H. Cowardin, and B. Buckalew (2015), “NIR Color vs Launch Date: A 20-year Analysis of Space Weathering Effects on the Boeing 376 Spacecraft,” Proceedings AMOS Conference, Maui HI.
7. E.C. Pearce et al. (2017), “Rapid Characterization of Geosynchronous Space Debris with 5-Color Near-IR Photometry,” Proceedings AMOS Conference, Maui HI.

8. M. Casali et al. (2007), "The UKIRT Wide-field Camera," Astronomy and Astrophysics, vol. 467, (2), pp. 777-784.

9. R. Howat et. al. (2004), "The Commissioning of and First Results from the UIST Imager Spectrometer," Proceedings of the SPIE, Astronomical Telescopes + Instrumentation, Glasgow UK, September 2004.

10. Ian R. Bryson, et. al. (1994), "Michelle, Mid-infrared Spectrometer and Imager." Proceedings of SPIE 2198.1, 715-24.

11. K. Jorgensen et. al. (2004), "Physical properties of orbital debris from spectroscopic observations," Advances in Space Research, 34, 1021-1025.

12. K. Abercromby, P. Abell, and E. Barker (2009), "Reflectance Spectra Comparison of Orbital Debris, Intact Spacecraft, and Intact Rocket Bodies in the GEO Regime," Proceedings of the Fifth European Conference on Space Debris, Darmstadt, Germany.

13. P. Seitzer *et. al.* (2012), "Visible Light Spectroscopy of GEO Debris,", Proceedings AMOS Conference, Maui HI.

14. D. Nishimoto et. al. (2001), " Spectroscopic observations of space objects and phenomena using Spica and Kala at AMOS," *Proceeding of the SPIE*, *International Symposium on Optical Science and Technology,* San Diego CA.

15. A. Vananti, T. Schildknecht, and H. Krag (2017), "Reflectance Spectroscopy Characterization of Space Debris," *Advances in Space Research,* 59: 2488-2500.

16. E. C. Pearce et al. (2020), "Examining the Effects of On-Orbit Aging of SL-12 Rocket Bodies using Visible Band Spectra with the MMT Telescope and 5-Color Photometry with the UKIRT/WFCAM," Journal of Space Safety Engineering 7.3: 376-80.

17. Gunter's Space Page, "Hughes/Boeing: HS-376/BSS-376," https://space.skyrocket.de/doc_sat/hs-376.htm, 2020.

18. "Mission Overview GE-6 Launch on the Proton Launch Vehicle," International Launch Services, 2000.

19. Gunter's Space Page, "Blok-D," http://space.skyrocket.de/doc_stage/blok-d.htm, 2020.

20. M. J. Currie, et al. (2014) "Starlink Software in 2013", *Astronomical Data Analysis Software and Systems XXIII*, 2014, vol. 485, p. 391.

21. T. Jenness, and F. Economou, "ORAC-DR: A generic data reduction pipeline infrastructure", *Astronomy and Computing*, vol. 9, pp. 40–48, 2015. doi:10.1016/j.ascom.2014.10.005.

22. H. Krantz, E.C. Pearce, L. Avner, O. Durney, C. Sauve, C. (2018). "Chimera: A high-speed three-color photometer for space surveillance and astronomy," *Proceedings of the SPIE, Astronomical Telescopes and Instrumentation*, Austin TX, 6 July 2018.

23. University of Arizona (2022), "Kuiper 61" Telescope", https://www.as.arizona.edu/kuiper-61-telescope, downloaded 16 August 2022.

24. J. Reyes *et. al.* (2018), "Characterization of spacecraft materials using reflectance spectroscopy,", Proceedings AMOS Conference, Maui HI.